

Evaluating GaN Doherty architectures for 4G Picocells, WiMax and microwave backhaul links

Original

Evaluating GaN Doherty architectures for 4G Picocells, WiMax and microwave backhaul links / R., Giofre; L., Piazzon; P., Colantonio; F., Giannini; Camarchia, Vittorio; Ghione, Giovanni; Pirola, Marco; Quaglia, Roberto. - STAMPA. - unico:(2014), pp. 1-6. (2014 IEEE 11th International Multi-Conference on Systems, Signals & Devices (SSD14) Castelldefels (Spagna) February 11 - 14) [10.1109/SSD.2014.6808832].

Availability:

This version is available at: 11583/2543424 since:

Publisher:

IEEE - INST ELECTRICAL ELECTRONICS ENGINEERS INC

Published

DOI:10.1109/SSD.2014.6808832

Terms of use:

This article is made available under terms and conditions as specified in the corresponding bibliographic description in the repository

Publisher copyright

(Article begins on next page)

Evaluating GaN Doherty Architectures for 4G Picocells, WiMax and Microwave Backhaul Links

R. Giofrè, L. Piazzon, P. Colantonio, F. Giannini
E.E. Dept. University of Roma Tor Vergata
Roma, ITALY
email: giofr@ing.uniroma2.it

V. Camarchia, G. Ghione, M. Pirola, R. Quaglia
DET-Politecnico di Torino
Torino, ITALY
email: roberto.quaglia@polito.it

Abstract— This paper evaluates the Doherty power amplifier architecture in terms of linearity, efficiency and design solutions. As case study four different prototypes are presented, one for 4G Picocells at 2.1 GHz, one for WiMax applications at 3.5 GHz and two for point-to-point microwave backhaul radiolinks at 7 GHz. Experimental results together with design guidelines are discussed addressing strengths and weaknesses of the Doherty architecture.

Index Terms—Doherty Amplifier, Efficiency, Linearity, Load Microwave link, Modulation, WCDMA, WiMax

I. INTRODUCTION

The increasing demand of high data rate services of modern wireless communication standards has affected the transmitter architecture. Spectral efficient communication standards have been introduced like the Code Division Multiple Access (CDMA), or the Orthogonal Frequency Division Multiplexing (OFDM). This has led to the revamping of topologies and architectural solutions able to fit the new scenario. From the Power Amplifiers (PAs) standpoint, the linearity and efficiency at back off have become the most important characteristics. Among the available solutions, one of the most adopted is today the Doherty Power Amplifier (DPA), both for handset and base station transmitters [1]-[3]. In the last few years it has been extensively studied and many solutions and innovations have been proposed [4]-[15]. For instance, outstanding performances have been obtained by properly controlling the higher harmonics [2]-[7]. Solutions for size reduction and to allow MMIC realization, even at lower frequencies, have been showed as well [5]. Besides, new circuit topologies have been proposed to improve DPA features such as: DPA with dual-band capabilities [8], DPA with a series-connected load [9], digitally driven dual-input DPA [10] and inverted DPA [12].

In this paper, an experimental evaluation of the Doherty linearity vs. efficiency trade-off is shown. As a case study, three designs are discussed: a 4G Picocell DPA at 2.1 GHz, a WiMax DPA at 3.5 GHz and a microwave backhaul radiolink DPA at 7 GHz.

II. DOHERTY PRINCIPLE OF OPERATION

As it is shown in Fig. 1, two amplifiers generally identified as Main and Auxiliary, an input splitter and a properly designed output combiner compose the classical DPA architecture.

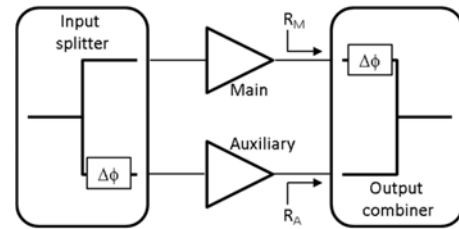


Fig. 1: Classical DPA schematic.

Independently on how these two passive networks are implemented, the DPA behavior as a function of the input power can be divided into two regions: the Doherty region, when both amplifiers are turned on, and back-off, when only the Main is active. The resulting efficiency behavior is characterized by two peaks with a high-efficiency region in the middle, as reported in Fig. 2.

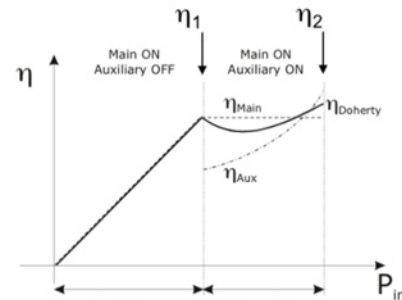


Fig. 2: Typical DPA efficiency behaviour.

Precisely, the first peak (η_1 in Fig. 2) occurs when the Main device reaches the maximum voltage swing across its drain terminal, while the Auxiliary amplifier is still off. The input power level, at which the Main amplifier reaches this operating condition, is usually referred as the DPA break point. The second peak (η_2 in Fig. 2) occurs when both

devices reach the maximum voltage swing at their drain terminals. The high efficiency region in between η_1 and η_2 is commonly referred as the output back-off (OBO) of the DPA.

Thanks to its efficiency *versus* output power behavior, the DPA represents a suitable candidate to realize amplification stages in systems working with time varying envelope signals. In fact, to maximize the instantaneous efficiency of the transmitter, the OBO of the DPA can be tuned according to the peak-to-average-power-ratio (PAPR) of the input signal. Besides the OBO value, other basic requirements of the DPA are: the RF carrier frequency (f_0), the peak output power level (P_{sat}) to be transmitted, and the required bandwidth (BW).

In order to obtain high efficiency levels in the OBO range, proper and accurate output loading conditions for both amplifiers at break and saturation have to be fulfilled. These loading conditions, R_M and R_A for Main and Auxiliary respectively, can be computed accounting for the design requirements and the active devices characteristics [16][17]:

$$R_{M@break} = \frac{(V_{DD} - V_k)^2}{2 \cdot \alpha^2 \cdot P_{sat}} \quad (1)$$

$$R_{M@sat} = \frac{(V_{DD} - V_k)^2}{2 \cdot \alpha \cdot P_{sat}} \quad (2)$$

$$R_{A@sat} = \frac{(V_{DD} - V_k)^2}{2 \cdot (1 - \alpha) \cdot P_{sat}} \quad (3)$$

where V_{DD} is the drain bias voltage and V_k is the device knee voltage, assumed to be the same for both devices. The parameter α is related to the OBO (defined in decibels) by:

$$\alpha^2 = \frac{P_{avg}}{P_{peak}} = \frac{1}{PAPR} = 10^{-\frac{OBO}{10}} \quad (4)$$

Once f_0 , P_{sat} , BW, OBO, V_{DD} and V_k have been evaluated, the output combiner and the input splitter of the DPA, together with the Main and Auxiliary matching networks, can be designed.

The output combiner ensures the correct loading conditions (1)-(3) in the entire BW. In the same frequency range, the input splitter has to assure the right splitting factor between the Main and Auxiliary devices. Moreover, both input/output splitter/combiner have to be tuned to allow the in-phase sum of the active devices' currents at the external termination (usually 50 Ω). Finally, the matching networks are required to compensate the parasitic elements of the active devices and, thus, to relax the requirements of the DPA splitter/combiner networks in the entire BW. A final remark on the fact that the passive networks have also to enforce the unconditional stability of the system.

III. DOHERTY FOR 4G PICOCCELL BASE STATIONS

Nowadays, smart-phones combine more advanced computing capability and connectivity than "old mobile

handsets", including features that are typical of personal computers. Therefore, mobile operators have to build network infrastructures to allow a fast and efficient mobile data exchange everywhere worldwide. In this scenario, picocell base stations for developing 4th generation (4G) networks are gaining traction [18]. Picocells are small versions of base stations, thus, they have to face the technical challenges of the 4G standard in terms of linearity and occupied bandwidth but with smaller footprint and lower output power level. Therefore, the efficiency and linearity trade-off in presence of high PAPR signals is a key aspect as well, and above all, in picocell base stations where power supply resources are limited. On the other hand, to fulfill a full interoperability within different standards, high performing PAs covering several RF bands represents a new frontier [19]. Hence, the search for novel solutions to implement wideband and/or multi-bands DPAs is becoming a key topic.

Here we discuss an original technique to improve the DPA efficiency versus frequency response [20]. The proposed approach is based on a different output-combining network. It is similar to a symmetrical branch-line with the fourth port in open circuit. If compared with a conventional approach, the novel combiner allows synthesizing an almost constant load for the Main device in a wider frequency range [21]. As a result, the DPA efficiency is less sensitive of frequency. The theoretical treatment of the novel output combiner is reported in [21], while a picture of the realized hybrid prototype is shown in Fig. 3. It is a 6 dB OBO DPA with 15% BW centered at 2.1 GHz and a saturated output power of 42 dBm. The used active device for both Main and Auxiliary amplifiers is a commercial 8W GaN HEMT (Cree CGH60008D).

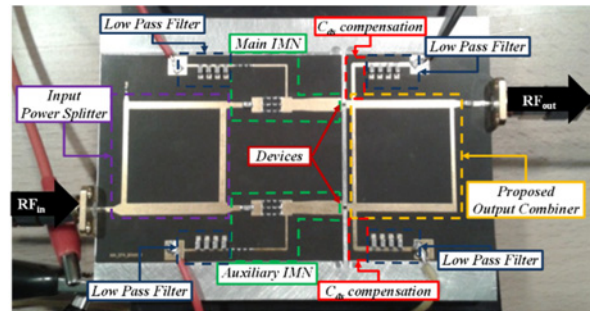


Fig. 3: Picture of the DPA for picocell base stations.

The passive networks were realized on a commercial substrate: Roger Duroid 5880. The drain bias voltage was set to 28-V for both PAs. The value of the optimum output resistance of the active device resulted to be $R_{OPT}=45.6 \Omega$, was inferred by performing Harmonic Balance simulations. Consequently, due to the 6 dB OBO, the output combiner has been designed to synthesize $R_{M@sat} = R_{A@sat} = R_{OPT}$ at the saturation and $R_{M@sat} = 2 \cdot R_{OPT} = 91.2 \Omega$ at 6-dB back-off power level. Thus, the characteristic impedances of the four $\lambda/4$ -TLs of the branch-line have been selected to fulfill such specifics resulting in $Z_{Horizontal}=36.6 \Omega$ and $Z_{Vertical}=54.1 \Omega$ [21].

Then, the Main and Auxiliary input matching networks, (IMNs) were designed. In this case, the same network was adopted for both devices. Finally, the uneven input power splitter (IPS) was designed to fulfill the required power-splitting ratio [17]. A branch-line coupler was adopted since it intrinsically allows the compensation of the 90° phase between the two amplifier's paths and shows a satisfactory bandwidth behavior. Moreover, it was designed to perform the input load transformation from $30\ \Omega$ to $50\ \Omega$, as well.

The quiescent current of the Main has been set to 20 mA (deep class AB) and the gate bias voltage of the Auxiliary (class C) has been adjusted to turn on at the 6 dB back-off power level. The active devices were connected to the passive networks by using three bond wires for each connection.

Fig. 4 shows the measured continuous wave performances versus frequency at the saturation ($P_{in}=33\text{dBm}$) and at 6-dB back-off ($P_{in}=27\text{dBm}$). As one can note, an efficiency in the range 65-51% has been registered for output power of 42–36.5-dBm and within the band 1.95 to 2.25 GHz.

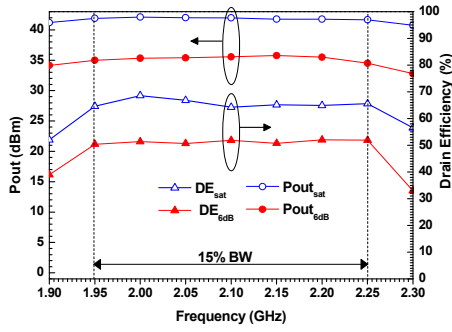


Fig. 4: Measured continuous wave performances vs. frequency.

The DPA has also been tested by using different complex signals. For instance, Fig. 5 shows the measured low and high adjacent channel power ratio (ACPR_{H/L}), efficiency, and gain behaviors as a function of the average output power when a 3GPP signal with 5.4-dB PAPR and 5-MHz video bandwidth around 2.1 GHz is used.

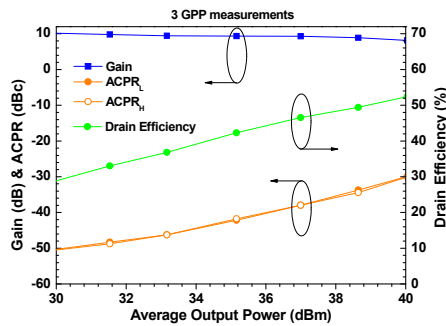


Fig. 5: DPA measured performances under 5-MHz 3GPP driving signal.

At 38 dBm of average output power, the average efficiency is around 50% with ACPR_{H/L} values lower than -35 dBc without any predistortion. The related measured normalized

output power spectrum is reported in Fig. 6. In order to further improve the linearity of the proposed architecture, a memory polynomial digital predistortion (DPD) function has been extracted from the real input-output measurements of the DPA [22][23]. The implemented function is similar to the one proposed in [24] with third and fifth order of memory depth and nonlinearity, respectively. The linearized spectrum is reported in Fig. 6 for comparison with the original one. As can be noted, DPD provides a substantial linearity improvement. In particular, 10 dBc ACPR_{H/L} improvement has been observed with final values lower than -45 dBc.

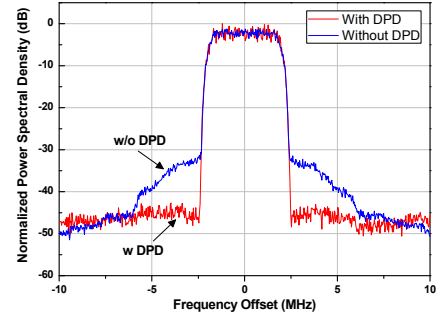


Fig. 6: DPA measured output power spectrum with 5-MHz 3GPP driving signal, before and after DPD.

IV. DOHERTY FOR WiMAX APPLICATIONS

WiMAX base-stations adopt, for the downlink channel, orthogonal frequency division multiplexing, which results in high-dynamic signals with large spectrum and high PAPR. As mentioned before, the DPA is well suited for realizing the PA in this scenario. In this particular realization designed for 3.5GHz WiMAX, a 2nd harmonic tuning design strategy for the main stage has been employed, while the auxiliary unit implements a class C power module. The adopted device is the CGH40010 from Cree inc., a packaged GaN HEMT on SiC with typical 10 W of $P_{OUT,1dB}$ in C-band, at a drain bias of 28V. With respect to tuned load approach [7], 2nd harmonic tuning allows the increasing of the fundamental drain voltage swing with respect of a class B amplifier [7]. The output power can therefore be increased of $\sqrt{2}$ times with respect to the tuned load case, positively affecting also the efficiency.

Thanks to their high breakdown voltage, GaN devices can implement this solution without decreasing the bias voltage of the device.

The strategy requires the optimization of the 2nd harmonic load termination (the 3rd harmonic is shorted), and the properly shaping of the input driving voltage (to adjust phase relations of the harmonics).

We applied the 2nd harmonic tuning to the main stage of the DPA, focusing on the performances optimization at the DPA break point, in order to maximize the efficiency in presence of a modulated signal. This has been obtained through careful non-linear simulations.

The main stage optimum load has resulted $R_{opt}=42\ \Omega$. The output matching network includes a $\lambda/4$ impedance transformer, while another $\lambda/4$ line has been inserted to match the external $50\ \Omega$ load. Broad-band unconditional stability has been enforced inserting RC networks at the input of both Main and Auxiliary cells. The fabricated amplifier has been mounted on a brass carrier, see Fig. 7.

The experimental characterization with CW single tone excitation at 3.5GHz [25] showed a satisfactory agreement between measurements and simulations, see Fig. 8, with measured drain efficiency higher than 55 % in a 6 dB OBO, together with a remarkably flat behavior.

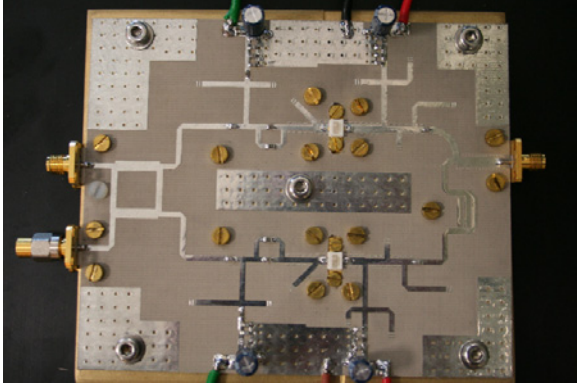


Fig. 7: Picture of the DPA for WiMax applications.

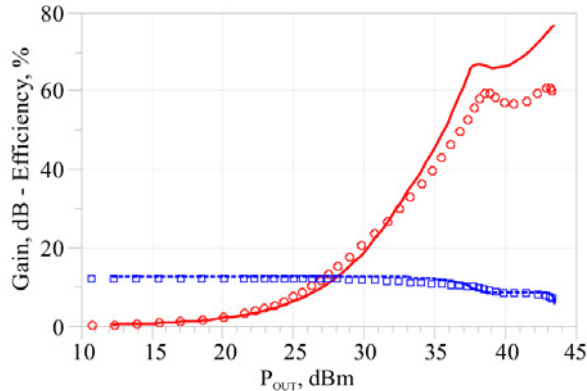


Fig. 8: DPA performances at 3.5 GHz CW driving signal. Gain (blue) and efficiency (red). Measurements (symbols) and simulations (solid lines).

The amplifier has been tested and linearized adopting a realistic WiMaX signal, with 7 MHz bandwidth and 9 dB of PAPR. The DPD has been designed through indirect learning approach adopting a Memory Polynomial (MP) scheme.

As evidenced in Fig. 9, DPD insertion allows to comply with the specifications of the standard, while the original spectrum exceeds the mask limits.

The shown spectra have been measured with an average output power of 34.2 dBm corresponding to 9 dB back-off with respect to the amplifier maximum power. The resulting average drain efficiency is around 40 %, corresponding to a PAE of 36 %.

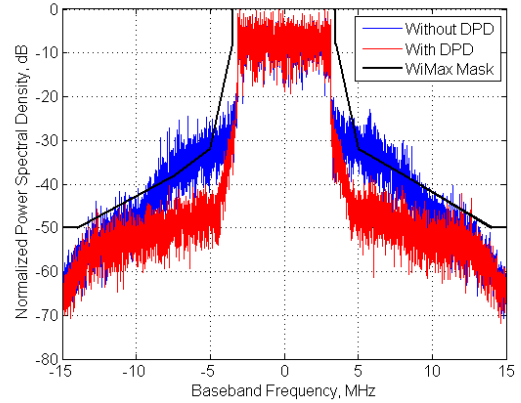


Fig. 9: Normalized output spectrum of the PA with (blue) and without (red) DPD, together with the WiMAX emission mask (black)

V. DOHERTY FOR MICROWAVE BACKHAUL LINK

The constant growth of services in mobile communications, such as web browsing, fast exchange of files and streaming video, is asking for an extremely high data transfer within each node of the global network. In this framework, backhaul links have to take part to the overall system evolution to avoid a bottleneck. Even if fiber optic backhaul links represent the preferable solution in terms of data transfer capability, microwave backhaul links still maintain their attractiveness for sites where the fiber optic approach cannot be exploited or efficiently implemented [26]. High data transfer on microwave physical layer can be achieved by using advanced signal-processing techniques that maximize the useful channel bandwidth. On the other hand, the adoption of sophisticated modulation schemes, e.g. high-order (256-, 512-, 1024-) QAM modulations, enables high data transfer rate, but also requires high linearity and efficiency transmitter units to correctly handle the high PAPR signals. Also in this scenario, the DPA can represent a suitable solution, above all when realized using GaN technology.

Here, we discuss two GaN MMIC DPAs for 7 GHz backhaul link infrastructures designed adopting two different strategies. The microscope pictures of the realized chips are shown in Fig. 10. The design of the MMIC in Fig. 10a) (DPA₁) is based on an asymmetrical class AB-C DPA solution [16][17]. The first design step is the identification of Main and Auxiliary device sizes. According to [27], if the DPA has 7 dB of OBO, the periphery ratio between Auxiliary and Main device must be around 2.6. Considering a drain bias voltage of 28V, the 4x100 μm and 10x100 μm devices have been adopted for Main and Auxiliary stages, respectively.

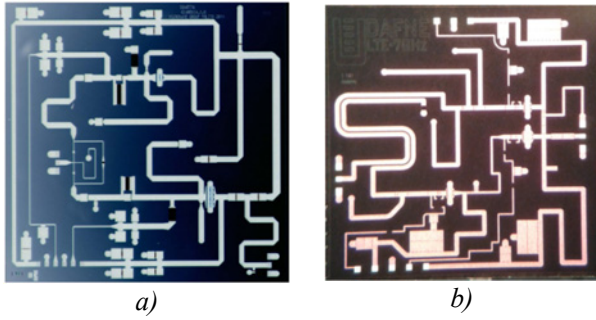


Fig. 10: Microscope pictures of the GaN MMIC DPAs for backhaul links

The former was biased in class AB ($V_{GG,M} = -3.2V$, $I_{D,M} = 40$ mA), while the latter in deep class C ($V_{GG,A} = -6.5$ V) conditions. Conversely, in the design of the MMIC in Fig. 10b) (DPA₂), a nonlinear driver stage is integrated in the Auxiliary branch to achieve a higher gain [28]. Moreover, a larger total periphery has been adopted to achieve a slightly greater output power than that one of DPA₁. In this case, $6 \times 100 \mu m$ and $6 \times 160 \mu m$ devices for Main and Auxiliary amplifiers were used, respectively. The Main was biased in class AB ($V_{GG,M} = -3.5V$, $I_{D,M} = 43$ mA) while the Auxiliary in class B ($V_{GG,A} = -4$ V). Same gate periphery ($6 \times 100 \mu m$) has been chosen for Main and Driver devices to ensure similar input load conditions for both DPA branches. Finally, the Driver was biased in class C ($V_{GG,D} = -4.6$ V) to assure the proper turning on condition of the Auxiliary branch.

The CW frequency behavior of the measured output power and efficiency at 3 dB of compression (a) and 7 dB of back-off (b), respectively, are reported in Fig. 11 [29].

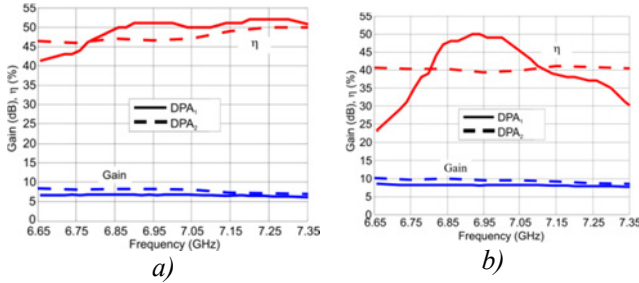


Fig. 11: Frequency behavior at 3 dB of gain compression (a) and at 7 dB of power back-off (b).

Results demonstrate an extremely flat output power behavior in 15% of bandwidth (6.35 GHz - 7.35 GHz) for the DPA₂, while in the entire bandwidth, a drain efficiency (PAE) higher than 40% (34%) at 7 dB of OBO has been registered. Conversely, the DPA₁ shows higher back-off efficiency, if compared with the DPA₂, in a 4% bandwidth around the center frequency, even if it exhibits rather fast degradation vs. frequency.

To evaluate the linearity performance of the two DPAs, system level analysis has been carried out, based on measured AM-AM and AM-PM static behaviours. The DPAs are tested with a signal with 56MHz channels spacing and 313 Mbit/s

capacity, whose spectrum emission mask is represented in Fig. 12. The DPAs, driven at average output power of 29 dBm (8 dB of OBO), show spectra slightly out-of-specification, but the needed linearity is expected to be recovered by the adoption of baseband predistortion [22][23].

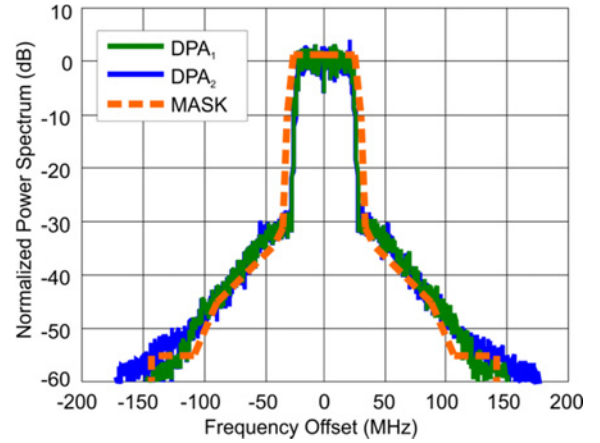


Fig. 12: Simulated spectrum from 29 dBm 256QAM signal generated from static AM/AM + AM/PM measurements at 7 GHz for DPA₁ (green) and DPA₂ (blue), compared to ETSI spectrum emission mask (orange dashed line).

VI. CONCLUSION

In this contribution, the Doherty PA design topology is shortly reviewed highlighting its key design steps. Three real field case study implementations are presented and discussed: 4G picocell systems, WiMax base stations and microwave backhaul links. The feasibility and the performance achievable by adopting the Doherty architecture are demonstrated.

ACKNOWLEDGEMENTS

This work was supported by the European Commission in the framework of the FP7 Network of Excellence in Wireless COMMunications NEWCOM# (Grant agreement no. 318306). The Microwave Engineering Center for Space Applications (M.E.C.S.A.) is also acknowledged.

REFERENCES

- [1] S. C. Cripps, "RF Power Amplifiers for Wireless Communication", Artech House, Nordwood, MA, 1999.
- [2] A. Grebennikov, S. Bulja, "High-Efficiency Doherty Power Amplifiers: Historical Aspect and Modern Trends," *Proceedings of the IEEE*, vol.100, no.12, pp.3190-3219, Dec. 2012.
- [3] R. Giofrè, L. Piazzon, P. Colantonio, F. Giannini, "Being seventy-five still young: the Doherty Power Amplifier" *Microwave Journal*, Vol. 55 Number: 4 April 2012, pp. 72-88.
- [4] P. Colantonio, F. Giannini, R. Giofrè, L. Piazzon; "Efficiency improvement in Doherty power amplifier by using Class F approach," *European Microwave Integrated Circuits Conference*, 2009. EuMIC 2009, pp.17-20, 28-29 Sept. 2009
- [5] D. Kang, J. Choi, D. Kim, D. Yu, K. Min, B. Kim "30.3% PAE HBT Doherty power amplifier for 2.5~2.7 GHz

- mobile WiMAX" 2010 *IEEE MTT-S Int. Microwave Symp. Dig.*, 2010, pp.796-799, June 2010.
- [6] P. Colantonio, F. Giannini, R. Giofrè, L. Piazzon, "GaN Doherty Amplifier With Compact Harmonic Traps," *Proceedings of the European Microwave Conference, EuMC 2008*, Amsterdam, The Netherlands, Oct. 2008, pp. 1553-1556.
 - [7] Jie Fang, J. Moreno, R. Quaglia, V. Camarchia, M. Pirola, S. Donati Guerrieri, C. Ramella, G. Ghione, "3.5 GHz WiMAX GaN Doherty power amplifier with second harmonic tuning" *Microw. And Optical Technology Letters*, vol.54, no.11, pp.2601-2605, Nov. 2012
 - [8] P. Colantonio, F. Feudo, F. Giannini, R. Giofrè, L. Piazzon, "Design of a Dual-Band GaN Doherty Amplifier" *Proceedings of XVIII International Conference on Microwaves, Radar and Wireless Communications MIKON 2010*, Lithuania, Vilnius, 14-16 June, Volume 2 pp.483-486
 - [9] S. Kawai, Y. Takayama, R. Ishikawa, K. Honjo, "A High-Efficiency Low-Distortion GaN HEMT Doherty Power Amplifier With a Series-Connected Load" *IEEE Trans. Microw. Theory & Tech.*, vol.60, no.2, pp.352-360, Feb. 2012
 - [10] R. Darraji, F. M. Ghannouchi, M. Helaloui, "Mitigation of Bandwidth Limitation in Wireless Doherty Amplifiers With Substantial Bandwidth Enhancement Using Digital Techniques," *IEEE Trans. Microw. Theory & Tech.*, vol.60, no.9, pp.2875-2885, Sept. 2012.
 - [11] P. Colantonio, F. Giannini, R. Giofrè, M. Piacentini, L. Piazzon, "A Design Approach to Increase Gain Feature of a Doherty Power Amplifier" *Proceedings of the 4th European Microwave Integrated Circuits Conference (EUMIC 2009)*, Roma, Italy, Set. 2009, pp. 25-28
 - [12] M.W. Lee, S. H. Kam, Y. S. Lee, Y. H. Jeong, "Design of Highly Efficient Three-Stage Inverted Doherty Power Amplifier" *IEEE Microw. and Wireless Compon. Lett.*, Vol. 21, no. 7, pp. 383-385, July 2011.
 - [13] P. Colantonio, F. Giannini, R. Giofrè, L. Piazzon "Simultaneous Dual-Band High Efficiency Harmonic Tuned Power Amplifier in GaN Technology" *2nd European Microwave Integrated Circuits 2007*. Munich, Germany, October 2007, EuMIC Conference Proceedings pp. 127-130.
 - [14] K. Bathich, A. Z. Markos, G. Boeck, "Frequency Response Analysis and Bandwidth Extension of the Doherty Amplifier," *IEEE Trans. Microw. Theory & Tech.*, vol.59, no.4, pp.934-944, April 2011.
 - [15] J. Moreno, Jie Fang, V. Camarchia, R. Quaglia, M. Pirola, G. Ghione, "3-3.6-GHz Wideband GaN Doherty Power Amplifier Exploiting Output Compensation Stages," *IEEE Trans. Microw. Theory & Tech.*, vol.60, no.8, pp.2543-2548, August 2012.
 - [16] P. Colantonio, F. Giannini, R. Giofrè, L. Piazzon, "Increasing Doherty amplifier average efficiency exploiting device knee voltage behavior," *IEEE Transactions on Microwave Theory and Techniques*, Vol. 59, N. 9, Sept. 2011, pp. 2295-2305
 - [17] P. Colantonio, F. Giannini, R. Giofrè, L. Piazzon, "The AB-C Doherty Amplifier: Part II Validation," *International Journal on RF and Microwave Computer-Aided Engineering* Volume 19 Issue 3 May 2009 Pages: 307-316 ISSN: 1096-4290 Copyright © 2009 Wiley Periodicals, Inc.
 - [18] M. Steer, "Beyond 3G," *IEEE Microwave Magazine*, IEEE, 2007, Vol. 8, pp. 76-82
 - [19] R. Fagotti, A. Cidronali, G. Manes, "Concurrent Hex-Band GaN Power Amplifier for Wireless Communication Systems," *Microwave and Wireless Components Letters*, IEEE, vol.21, no.2, pp.89,91, Feb. 2011.
 - [20] R. Giofrè, P. Colantonio, F. Giannini, and L. Piazzon, "New output combiner for doherty amplifiers," *IEEE Microw. and Wireless Compon. Lett.*, vol. 23, no. 1, pp. 31-33, Jan. 2013.
 - [21] R. Giofrè, L. Piazzon, P. Colantonio, F. Giannini, "A Doherty Architecture with High Feasibility and Defined Bandwidth Behavior," *IEEE Transactions on Microwave Theory and Techniques*, Vol. 61, N. 9, Sept. 2013, pp. 3308-3317.
 - [22] R. Quaglia, V. Camarchia, S. Guerrieri, E. Lima, G. Ghione, Q. Luo, M. Pirola, and R. Tinivella, "Real-time FPGA-based baseband predistortion of W-CDMA 3GPP high-efficiency power amplifiers: Comparing GaN HEMT and Si LDMOS predistorted PA performances," in *Microwave Conference, 2009. EuMC 2009. European*, Oct. 2009, pp. 342-345.
 - [23] F. Ghannouchi and O. Hammi, "Behavioral modeling and predistortion," *IEEE Microw. Mag.*, vol. 10, no. 7, pp. 52-64, Dec.
 - [24] D. Morgan, Z. Ma, J. Kim, M. Zierdt, and J. Pastalan, "A generalized memory polynomial model for digital predistortion of RF power amplifiers," *IEEE Trans. Signal Process.*, vol. 54, no. 10, pp. 3852-3860, Oct. 2006.
 - [25] V. Camarchia, V. Teppati, S. Corbellini, and M. Pirola, "Microwave Measurements-Part II Non-linear Measurements," *IEEE Instrum. Meas.Mag.*, vol. 10, no. 3, pp. 34-39, Jun. 2007.
 - [26] Hansryd, J. and Edstam, J.: 'Microwave capacity evolution', *Ericsson Rev. J.*, 2011,
 - [27] V. Camarchia, J. Fang, J. Moreno Rubio, M. Pirola, and R. Quaglia, "7 GHz MMIC GaN Doherty Power Amplifier with 47% efficiency at 7 dB output back-off," *IEEE Microw. Wireless Compon. Lett.*, vol. 23, no. 1, pp. 34-36, Jan. 2013.
 - [28] L. Piazzon, P. Colantonio, F. Giannini, R. Giofrè, "15% Bandwidth 7GHz GaN-MMIC Doherty Amplifier With Enhanced Auxiliary Chain" "Accepted for publication in *Microwave and Optical Technology Letters*, 2013 Wiley Periodicals.
 - [29] V. Camarchia, J. Moreno, M. Pirola, R. Quaglia, P. Colantonio, F. Giannini, R. Giofrè, L. Piazzon, T. Emanuelsson, T. Wegeland, "High-Efficiency 7 GHz Doherty GaN MMIC Power Amplifiers for Microwave Backhaul Radio Links," *Electron Devices, IEEE Transactions on*, vol. 60, no. 10, pp. 3592-3595, Oct. 2013.